J. Phys. Chem. A **2006,** *110,* 8151−8157

Oxidation Pattern of Small Silicon Oxide Clusters: Structures and Stability of Si_6O_n ($n = 1-12$)

Q. J. Zang,[†,‡] **Z. M. Su,***[,†,§] **W. C. Lu,***[,‡,⊥,||] **C. Z. Wang,**[⊥] **and K. M. Ho**[⊥]

Institute of Functional Material Chemistry, Northeast Normal University, Changchun 130024, P. R. China,
State Key Laboratory of Theoretical and Computational Chemistry, Jilin University, Changchun 130021,
P. R. China, and Ames Laboratory—U.S. DOE and Department of Physics and Astronomy,
Iowa State University, Ames, Iowa 50011

Received: March 12, 2006

We have performed systematic ab initio calculations to study the structures and stability of Si_6O_n clusters ($n = 1-12$) in order to understand the oxidation process in silicon systems. Our calculation results show that oxidation pattern of the small silicon cluster, with continuous addition of O atoms, extends from one side to the entire Si cluster. Si atoms are found to be separated from the pure Si cluster one-by-one by insertion of oxygen into the Si−O bonds. From fragmentation energy analyses, it is found that the Si-rich clusters usually dissociate into a smaller pure Si clusters (Si_5, Si_4, Si_3, or Si_2), plus oxide fragments such as SiO, Si_2O_2, Si_3O_3, Si_3O_4, and Si_4O_5. We have also studied the structures of the ionic $Si_6O_n^{\pm}$ ($n = 1-12$) clusters and found that most of ionic clusters have different lowest-energy structures in comparison with the neutral clusters. Our calculation results suggest that transformation $Si_6O_n^{+}(\mathbf{a}) + O \rightarrow Si_6O_{n+1}^{+}(\mathbf{a})$ should be easier.

I. Introduction

Because of the importance of silicon oxide materials in science and technology and the important role of silicon oxide in the recent chemical vapor deposition growth of silicon nanowires and nanostructures, silicon oxide clusters have attracted more and more attention both from experimental[1−8] and theoretical[9−15] studies in recent years.

Using photoelectron spectroscopy, small anionic silicon oxide clusters such as Si_3O_n ($n = 1-6$) has been investigated by Wang and co-workers.[1,2] Their results provide very useful information on the electronic properties and structure assignment of these small Si_3O_n clusters. Experimental studies of reaction of silicon clusters with oxygen have been performed by Creasy et al. and by Jarrold et al.[3,4] Creasy and co-workers[3] studied the reactions of cationic silicon clusters containing up to six atoms with oxygen. Their study shows that the small cationic silicon clusters were etched away by the oxidation reaction, two silicon atoms at a time, all the way down to Si_2^+ or Si^+. Jarrold and co-workers studied the chemical reactions of medium-sized ionic silicon clusters, Si_n^+ ($n = 10-65$) with oxygen.[4] Their experimental results suggested that for clusters containing fewer than 29 atoms, the main products were found to be Si_{n-2}^+ and two SiO molecules. Each reaction of an oxygen molecule with the silicon cluster results in the loss of two Si atoms in two SiO radicals. Bergeron and Castleman Jr. has also studied the stability of silicon cluster ions by O_2 etching, suggesting that Si_n^+ ($n = 4, 6, 9, 13, 14$, and 23) and Si_n^- ($n = 18, 21, 24, 25$, and 28) have very large stability.[5] Recently, the experimental study on the oxidation of the Si nanostructures has also been performed, suggesting that the reactivity of oxygen with Si nanostructures is relatively low, and imposes some restriction on the oxidation of Si films.[7]

On the theory side, ab initio calculations of small Si_nO_m with $n \leq 5$ clusters have been carried out to study the structures and potential energy surfaces of small silicon oxide clusters in great detail. Chelikowsky and co-workers have investigated the geometric structures and electronic properties of neutral and charged Si_nO_n ($n = 3$, 4, and 5) clusters.[9] Their computational results suggested that buckled rings are more stable than planar ones for Si_4O_4 and Si_5O_5. Lu and co-workers have studied systematically the structures and fragmentation stabilities of Si_mO_n ($m = 1-5$, $n = 1-(2m + 1)$) clusters.[10] In their work, energetically favorable structures of silicon oxide clusters were proposed and the fragmentation pathways of small silicon oxide clusters were also analyzed, showing that SiO is the most abundant species in the fragmentation products, consistent with the experiment results.[16,17] Recently, ab initio calculations of larger silicon oxide clusters with O/Si ratios of 2:1 (Si_nO_{2n}) and 1:1 (Si_nO_n) have also been reported,[18−20] while the studies of medium-sized silicon dioxide clusters[18,19] provide useful information on the most stable motif of silicon dioxide clusters, the studies of medium-sized silicon monoxide clusters[20] especially aimed at understanding the nucleation mechanism in the growth of silicon-based nanostructures at the atomic level.

Most of the previous studies (except for ref 10) were focused on O-rich silicon oxide clusters while information about the Si-rich clusters which is important for understanding the growth mechanism of the silicon nanostructures is still lacking. Understanding the structural character of Si-rich clusters and the difference between Si- and O-rich cluster structures is highly desirable. Although a detailed study for Si_mO_n ($m = 1-5$, $n = 1-(2m + 1)$) clusters has been reported,[10] the systems contain-

---

[*] Corresponding authors.

[†] Institute of Functional Material Chemistry, Northeast Normal University.

[‡] State Key Laboratory of Theoretical and Computational Chemistry, Jilin University.

[§] E-mail: suzm@nenu.edu.cn.

[⊥] Ames Laboratory—U.S. DOE and Department of Physics and Astronomy, Iowa State University.

[||] E-mail: wencailu@jlu.edu.cn.

10.1021/jp061517l CCC: $33.50

ing only up to five Si atoms is still too small to provide clear information on the oxidation process and the comparison between Si-rich and O-rich clusters.

In this paper, we have performed a systematic study to investigate the structure and stability of Si_6O_n ($n = 1-12$) neutral and ionic clusters. Our purposes are 3-folds: (i) To compare the structures of Si_6O_n clusters at different O/Si ratios, and to investigate the oxidation process of small silicon oxide clusters with continuous addition of O atoms. (ii) To estimate the relative stability of Si_6O_n clusters according to binding energies and fragmentation energies. (iii) To study the structures of ionic Si_6O_n clusters and compare with the neutral ones. To our knowledge, there have been much less theoretical studies on the small ionic silicon oxide clusters. However, in experiments charged clusters are usually involved.

II. Computational Methods

Our calculations were performed using the GAUSSIAN 03 package[21] at the level of first-principles density functional theory (DFT) with generalized gradient approximation (GGA) of B3LYP functional[22] for the exchange-correlation energy and with the 6-311G(2d) basis set. The cluster structures were optimized without any symmetry constraints. Lowest-energy structures of Si_6O_n ($n = 1-12$) clusters were located from as many as possible initial structures constructed based on chemical bonding estimation and our experience in the previous study of Si_mO_n ($m = 1-5$, $n = 1-(2m + 1)$) clusters. Such a time-exhaustive search is doable for small clusters. To confirm the stability of lowest-energy structures, frequency analyses of neutral Si_6O_n ($n = 1-12$) clusters were also examined.

III. Results and Discussion

For each Si_6O_n ($n = 1-12$) cluster, three lowest-energy isomers are shown in Figure 1. The structural difference between Si-rich and O-rich clusters can be seen from the plot as we will discuss in the following. Variation of structure motif with O/Si ratio for the silicon oxides Si_6O_n ($n = 1-12$) provide useful information for understanding the oxidation pattern of small silicon clusters.

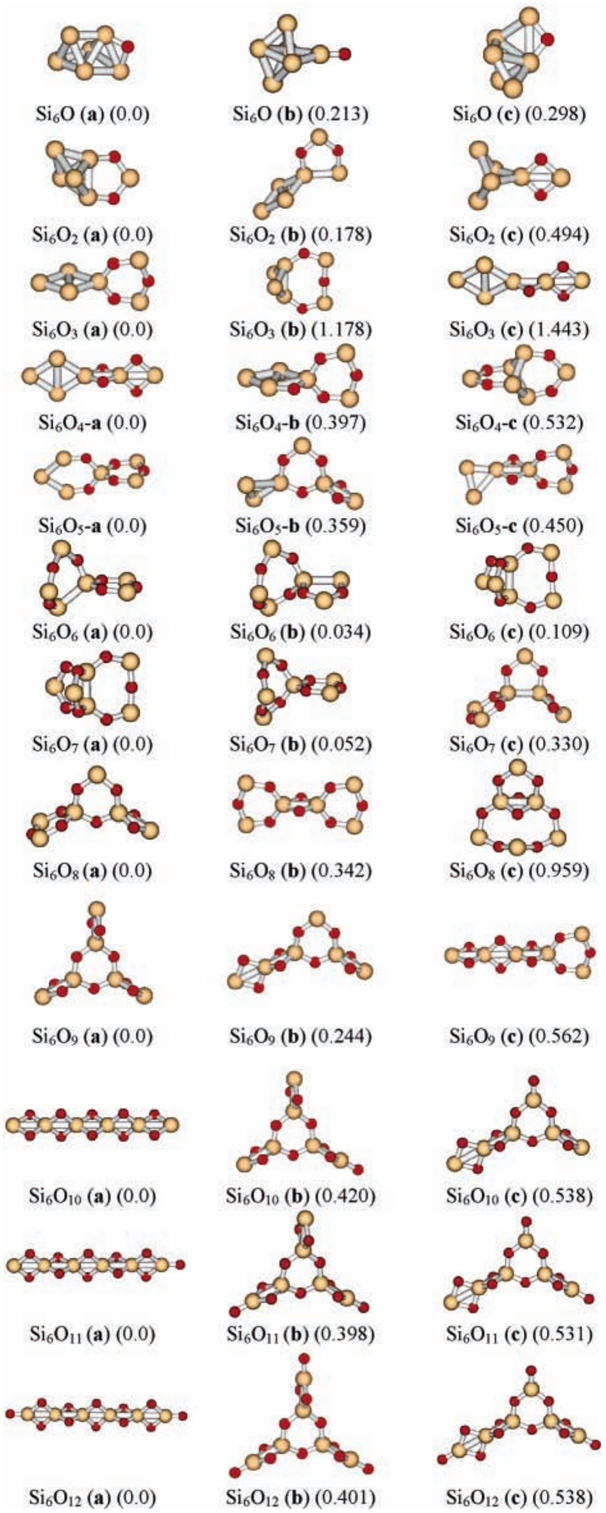

Si_6O (**a**) (0.0) Si_6O (**b**) (0.213) Si_6O (**c**) (0.298)

Si_6O_2 (**a**) (0.0) Si_6O_2 (**b**) (0.178) Si_6O_2 (**c**) (0.494)

Si_6O_3 (**a**) (0.0) Si_6O_3 (**b**) (1.178) Si_6O_3 (**c**) (1.443)

Si_6O_4-**a** (0.0) Si_6O_4-**b** (0.397) Si_6O_4-**c** (0.532)

Si_6O_5-**a** (0.0) Si_6O_5-**b** (0.359) Si_6O_5-**c** (0.450)

Si_6O_6 (**a**) (0.0) Si_6O_6 (**b**) (0.034) Si_6O_6 (**c**) (0.109)

Si_6O_7 (**a**) (0.0) Si_6O_7 (**b**) (0.052) Si_6O_7 (**c**) (0.330)

Si_6O_8 (**a**) (0.0) Si_6O_8 (**b**) (0.342) Si_6O_8 (**c**) (0.959)

Si_6O_9 (**a**) (0.0) Si_6O_9 (**b**) (0.244) Si_6O_9 (**c**) (0.562)

Si_6O_{10} (**a**) (0.0) Si_6O_{10} (**b**) (0.420) Si_6O_{10} (**c**) (0.538)

Si_6O_{11} (**a**) (0.0) Si_6O_{11} (**b**) (0.398) Si_6O_{11} (**c**) (0.531)

Si_6O_{12} (**a**) (0.0) Si_6O_{12} (**b**) (0.401) Si_6O_{12} (**c**) (0.538)

Figure 1. Structures of three lower-energy isomers for neutral Si_6O_n ($n = 1-12$) clusters, calculated at B3LYP/6-311G(2d).

A. Structures. Si-Rich Clusters Si_6O_{1-5}. As shown in Figure 1, the lowest-energy isomer we obtained for Si_6O cluster is the isomer Si_6O(**a**) in which the O forms a bridge with two Si atoms in the Si_6 cluster. Such a structure is more stable than the $>Si{=}O$ structure of isomer **b** as well as another O bridge structure of isomer **c**. Note that in Si_6O, no Si atom has been separated from the Si_6 cluster. For Si_6O_2 cluster, the best structure we obtained is the isomer Si_6O_2(**a**), which contains a SiO_2 unit arched to the most stable structure of a pure Si_5 cluster. Higher-energy isomer **b** consists of a Si_4 and a Si_3O_2 unit sharing a Si atom, and isomer **c** contains a Si_2O_2 unit. Note that in Si_6O_2, one Si atom has been separated from the pure Si cluster by the insertion of two oxygen atoms. The lowest-energy structure for Si_6O_3 is a very stable structure consisted of a Si_4 and a Si_3O_3 fragments sharing a Si atom. The Si_4 and Si_3O_3 ring structures have been shown to be the units with special stability, and as a result, their combination leads to a very stable structure Si_6O_3-(**a**). Two Si atoms in Si_6O_3 have been separated from the pure Si cluster by the oxidation of three oxygen atoms. For Si_6O_4, the lowest-energy structure is an assembly of a Si_4 and a Si_3O_4 unit with a common Si atom connecting these two units. In our previous study, the double-O bridged structure of Si_3O_4 is shown to be the most stable geometry. Here we see that the lower-energy blocks of silicon clusters and silicon oxide clusters can get together to form an energetically stable structure. Here, two Si atoms have been separated from the original Si_6 cluster by four oxygen atoms. For Si_6O_5, the lowest-energy structure Si_6O_5-(**a**) is a two-ring structure containing a pure Si_3 unit located at one end, the rest of Si atoms are oxidized. From this systematic study, it can be seen that oxidation of small Si cluster proceeds from one end of the cluster and extends to entire clusters as the O/Si ratio approaches 1. We also found that simultaneous etching from both side of the Si_6 cluster such as Si_6O_4(**c**) and other tested structures not shown in Figure 1 are less favorable. There exists a clear boundary between the oxidized and the nonoxidized parts, and the pure Si cluster does exist until the O atom number reaches approximately the Si atom number, i.e., at about O/Si ≈ 1:1 ratio.

Si_6O_6 and Si_6O_7. Si_6O_n clusters with O/Si ratios close to 1 are the transition stage from Si-rich to O-rich systems. Our calculation results show that Si_6O_6 favors a two-ring structure, and Si_6O_7 trends to take a three-ring framework. As we have shown in our previous study,[10] the Si_4O_4 ring is the largest monocycle Si_nO_n ring that can be stabilized. For Si_5O_5, a two-ring structure is already energetically more favorable than the single-ring structure. Monoxide clusters such as Si_6O_6 have attracted more attention recently since they are believed to have smaller HOMO−LUMO gap and larger reactivity, thus may play an important role in the growth of silicon nanomaterials.[20] Our calculation results show that the Si_6O_n clusters with O:Si ratio close to 1 are indeed less stable in view of their smaller binding energies and smaller fragmentation energies which will be discussed below.

O-Rich Clusters Si_6O_{8-12}. For the Si_6O_8 cluster, the lowest-energy structure we obtained is an assembly of two Si_3O_3 rings and one Si_2O_2 ring with two shared Si atoms at the points of intersections. This structure is more stable than Si_6O_8 isomer **b** where the Si_2O_2 ring bridges two Si_3O_3 rings, or isomer **c** where Si_2O_2 is located inside three Si_3O_2 rings. With an O atom addition to Si_6O_8, the stable structure of Si_6O_9 cluster has a framework of one Si_3O_3 ring at the center connected by three Si_2O_2 ligands. This structure is more stable than isomers **b** and **c**, where a chain of two or three Si_2O_2 rings is formed, suggesting that the double-O bridged ($-Si_2O_2-$) structure is less favorable due to its large strain energy. From Si_6O_{10} to Si_6O_{11} to Si_6O_{12}, the lowest-energy structures are all double-oxygen-bridged ($-Si_2O_2-$) structures, similar to the cases of smaller dioxide clusters Si_nO_{2n} for $n = 2-5$. Even with a large strain energy, the Si_2O_2 building block is still more favorable than the structure with dangling Si═O bond. This result suggests that for silicon oxide systems, Si atoms prefer to interact with neighboring O atoms to form tetrahedral *sp*3 hybrid bonds other than planar sp^2 hybrid bonds. It should be pointed out that although the double-oxygen-bridged ($-Si_2O_2-$) structures are favorable for smaller silicon dioxide clusters Si_nO_{2n} ($n = 2-6$), a 2D ring structure formed by the Si_2O_2 will become more stable when silicon oxide clusters getting bigger.[15]

Ionic Clusters $Si_6O_n^+$ and $Si_6O_n^-$. On the basis of the structures of the neutral Si_6O_n clusters, we have performed further calculations to study the structures of cationic and anionic clusters $Si_6O_n^+$ and $Si_6O_n^-$ ($n = 1-12$). To search for the favorable structures of the ionic clusters, several lower-energy isomers of each size of neutral Si_6O_n clusters were selected as initial structures and then optimized by ab initio calculations with the addition of one positive or one negative charge. Three lower-energy structures for each size of the cationic and anionic clusters, shown in the order **a**, **b**, and **c**, are plotted in Figure 2 and Figure 3, respectively. For the ionic Si-rich clusters, their lowest-energy structures are mostly different from those of the corresponding neutral clusters. For the Si_6O neutral and ionic clusters, Si_6O^-(**a**) (Figure 3) is similar to Si_6O(**a**) (Figure 1), while Si_6O^+(**a**) (Figure 2) is similar to Si_6O(**c**) (Figure 1). The lowest-energy structures $Si_6O_2^+$(**a**) and $Si_6O_2^-$(**a**) were resulted from Si_6O_2(**b**) and Si_6O_2(**c**), respectively, both are different from the Si_6O_2(**a**) structure. For $Si_6O_3^{\pm}$, the most stable structures are similar to the neutral structure Si_6O_3(**a**), except that the Si_4 fragment in $Si_6O_3^-$(**a**) is buckled other than planar. We can see that the Si_6O_3(**a**) structure with a combination of Si_4 and Si_3O_3 units is very stable even with adding or losing one electron.

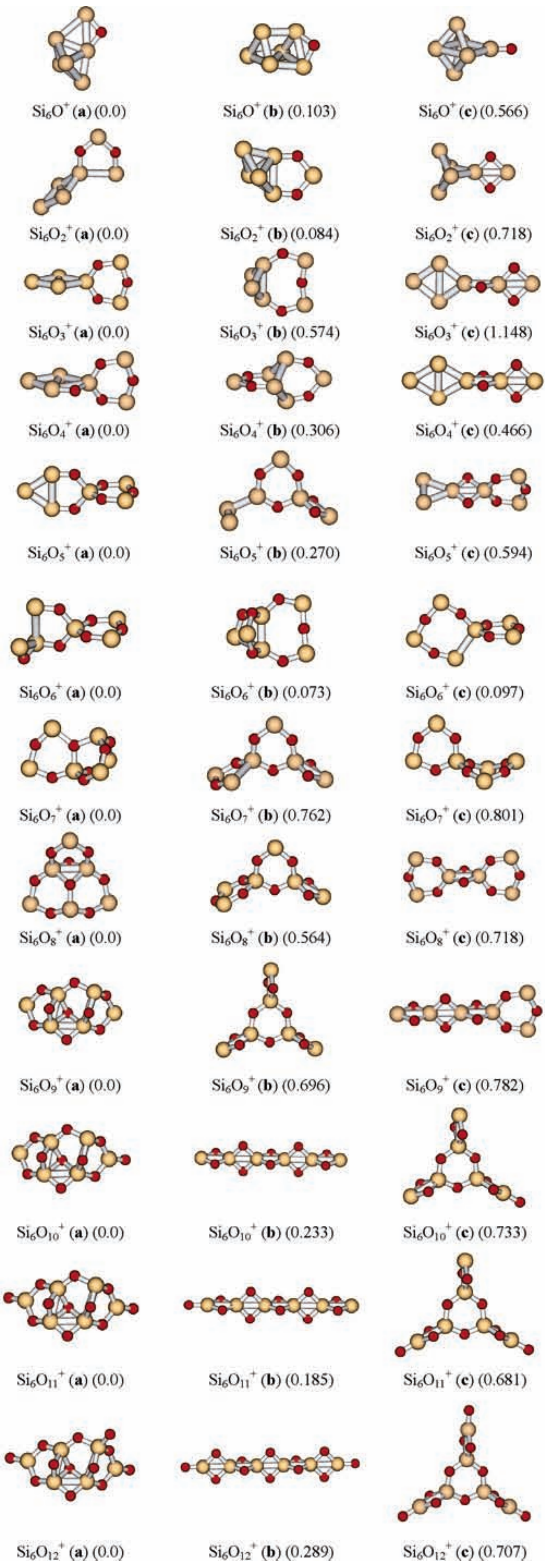
Si_6O^+ (**a**) (0.0) Si_6O^+ (**b**) (0.103) Si_6O^+ (**c**) (0.566)
$Si_6O_2^+$ (**a**) (0.0) $Si_6O_2^+$ (**b**) (0.084) $Si_6O_2^+$ (**c**) (0.718)
$Si_6O_3^+$ (**a**) (0.0) $Si_6O_3^+$ (**b**) (0.574) $Si_6O_3^+$ (**c**) (1.148)
$Si_6O_4^+$ (**a**) (0.0) $Si_6O_4^+$ (**b**) (0.306) $Si_6O_4^+$ (**c**) (0.466)
$Si_6O_5^+$ (**a**) (0.0) $Si_6O_5^+$ (**b**) (0.270) $Si_6O_5^+$ (**c**) (0.594)
$Si_6O_6^+$ (**a**) (0.0) $Si_6O_6^+$ (**b**) (0.073) $Si_6O_6^+$ (**c**) (0.097)
$Si_6O_7^+$ (**a**) (0.0) $Si_6O_7^+$ (**b**) (0.762) $Si_6O_7^+$ (**c**) (0.801)
$Si_6O_8^+$ (**a**) (0.0) $Si_6O_8^+$ (**b**) (0.564) $Si_6O_8^+$ (**c**) (0.718)
$Si_6O_9^+$ (**a**) (0.0) $Si_6O_9^+$ (**b**) (0.696) $Si_6O_9^+$ (**c**) (0.782)
$Si_6O_{10}^+$ (**a**) (0.0) $Si_6O_{10}^+$ (**b**) (0.233) $Si_6O_{10}^+$ (**c**) (0.733)
$Si_6O_{11}^+$ (**a**) (0.0) $Si_6O_{11}^+$ (**b**) (0.185) $Si_6O_{11}^+$ (**c**) (0.681)
$Si_6O_{12}^+$ (**a**) (0.0) $Si_6O_{12}^+$ (**b**) (0.289) $Si_6O_{12}^+$ (**c**) (0.707)

Figure 2. Structures of three lower-energy isomers for cationic $Si_6O_n^+$ ($n = 1-12$) clusters, calculated at B3LYP/6-311G(2d).

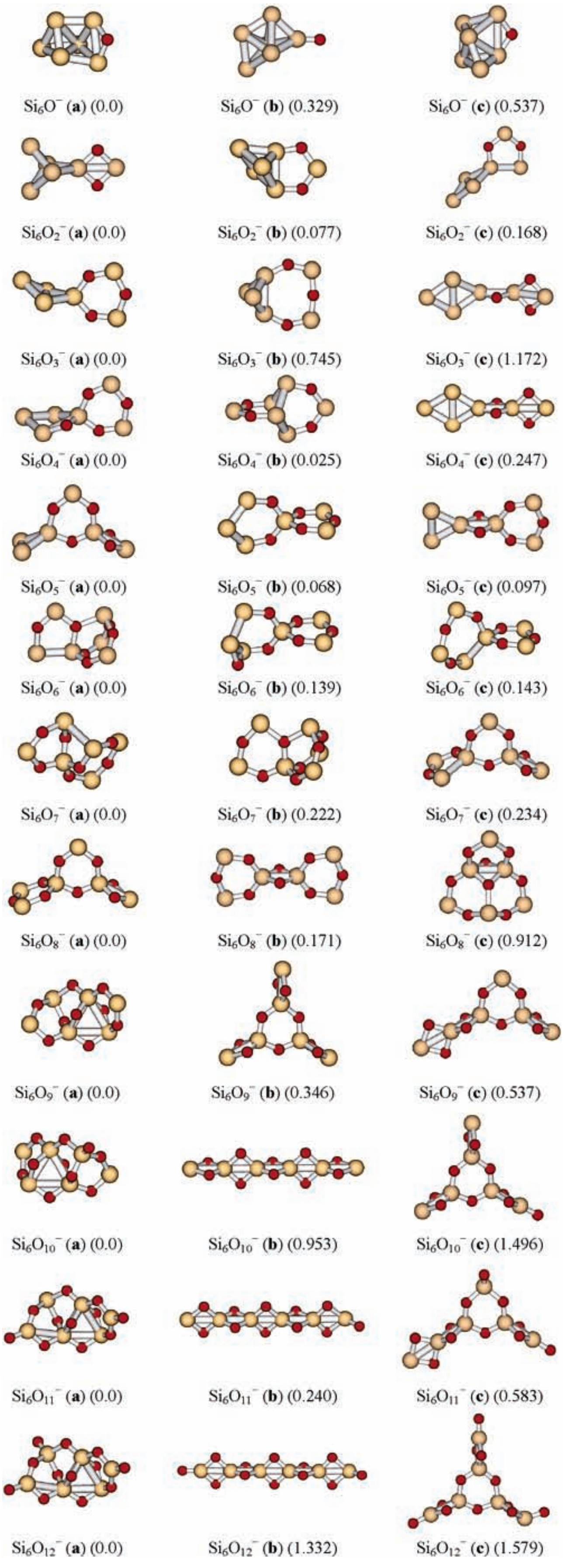

Si_6O^- **(a)** (0.0) Si_6O^- **(b)** (0.329) Si_6O^- **(c)** (0.537)

$Si_6O_2^-$ **(a)** (0.0) $Si_6O_2^-$ **(b)** (0.077) $Si_6O_2^-$ **(c)** (0.168)

$Si_6O_3^-$ **(a)** (0.0) $Si_6O_3^-$ **(b)** (0.745) $Si_6O_3^-$ **(c)** (1.172)

$Si_6O_4^-$ **(a)** (0.0) $Si_6O_4^-$ **(b)** (0.025) $Si_6O_4^-$ **(c)** (0.247)

$Si_6O_5^-$ **(a)** (0.0) $Si_6O_5^-$ **(b)** (0.068) $Si_6O_5^-$ **(c)** (0.097)

$Si_6O_6^-$ **(a)** (0.0) $Si_6O_6^-$ **(b)** (0.139) $Si_6O_6^-$ **(c)** (0.143)

$Si_6O_7^-$ **(a)** (0.0) $Si_6O_7^-$ **(b)** (0.222) $Si_6O_7^-$ **(c)** (0.234)

$Si_6O_8^-$ **(a)** (0.0) $Si_6O_8^-$ **(b)** (0.171) $Si_6O_8^-$ **(c)** (0.912)

$Si_6O_9^-$ **(a)** (0.0) $Si_6O_9^-$ **(b)** (0.346) $Si_6O_9^-$ **(c)** (0.537)

$Si_6O_{10}^-$ **(a)** (0.0) $Si_6O_{10}^-$ **(b)** (0.953) $Si_6O_{10}^-$ **(c)** (1.496)

$Si_6O_{11}^-$ **(a)** (0.0) $Si_6O_{11}^-$ **(b)** (0.240) $Si_6O_{11}^-$ **(c)** (0.583)

$Si_6O_{12}^-$ **(a)** (0.0) $Si_6O_{12}^-$ **(b)** (1.332) $Si_6O_{12}^-$ **(c)** (1.579)

Figure 3. Structures of three lower-energy isomers for anionic $Si_6O_n^-$ ($n = 1-12$) clusters, calculated at B3LYP/6-311G(2d).

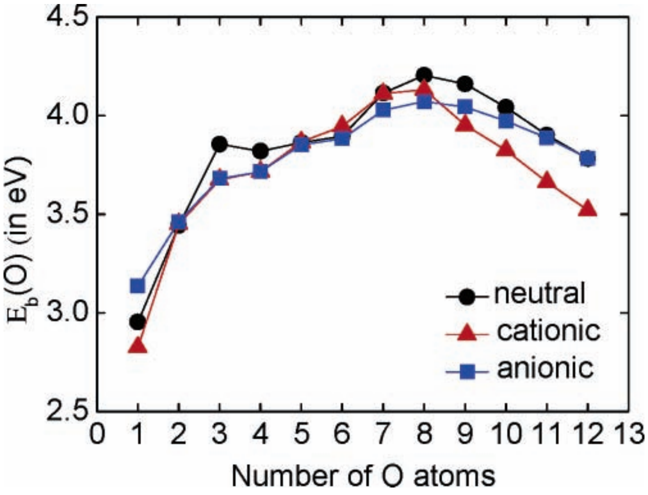

Figure 4. Binding energies per O atom by eqs 1−3 for $Si_6O_n^{0,\pm}$(**a**) ($n = 1-12$) clusters, calculated at B3LYP/6-311G(2d).

For Si_6O_4 ionic clusters, the lowest-energy structures $Si_6O_4^+$(**a**) and $Si_6O_4^-$(**a**) correspond to Si_6O_4(**b**). $Si_6O_4^\pm$(**c**), optimized from Si_6O_4(**a**) with Si_4 and a double-oxygen bridged units, are less stable. $Si_6O_5^+$(**a**) is similar to Si_6O_5(**a**), but $Si_6O_5^-$(**a**) corresponds to Si_6O_5(**b**). For Si_6O_6 and Si_6O_7 ionic clusters, $Si_6O_6^+$(**a**) and $Si_6O_6^-$(**a**) were obtained from a neutral isomer with a similar structure and Si_6O_6(**b**), respectively, and $Si_6O_7^+$(**a**) and $Si_6O_7^-$(**a**) from Si_6O_7(**b**). We can see that the anionic $Si_6O_6^-$ and $Si_6O_7^-$ structures are much more distorted compared with the corresponding neutral isomers.

$Si_6O_8^+$ has a stable structure corresponding to Si_6O_8(**c**). $Si_6O_8^-$ has a lowest-energy structure similar to the neutral structure Si_6O_8(**a**). For over-O-rich clusters, Si_6O_9 to Si_6O_{12}, all the ionic clusters, either cationic or anionic ones, have lowest-energy structures different from the corresponding neutral clusters. Therefore, the structures of over-O-rich clusters, Si_6O_9 to Si_6O_{12}, are less stable upon adding or losing one electron.

B. Oxidation Motif of Silicon Oxide Clusters. The survey of $Si_6O_n^{0,\pm}$ lowest-energy structures with n ranging from 1 to 12 displays a feature of oxidation pattern in the small silicon oxide clusters. The oxidation starts from one end of silicon clusters and etches Si atoms continuously going through to the other end of clusters. Two-way oxidation process with pure Si fragment located at the center is less favorable, e.g., Si_6O_4(**c**) and other tested structures which are higher in energy and not shown in Figures 1−3. For Si-rich clusters, the lowest-energy structures are composed of two fragments: one pure silicon fragment (e.g., Si_5, Si_4, and Si_3 units) and the other silicon oxide fragment (e.g., Si_2O_2, Si_3O_3, Si_3O_4, etc.), with a clear boundary between the two units. When the O/Si ratio in the cluster reaches 1 or slightly larger, e.g., Si_6O_6, and Si_6O_7, almost all Si atoms in the cluster are oxidized. Small silicon oxide clusters with the O/Si $\approx$ 1:1 ratio can be considered as a transition point between Si-rich and O-rich clusters. Among the O-rich clusters, the lowest-energy structures have similar disklike motif for Si_6O_8 and Si_6O_9, however with adding one more O atom, there is an apparent motif transition from the disklike structure to the double-oxygen-bridged rod structure in order to accommodate more O atoms.

From the studies of the ionic clusters $Si_6O_n^\pm$, we found that the addition of O atoms to cationic clusters $Si_6O_n^+$(**a**) can readily lead to the next most stable structures $Si_6O_{n+1}^+$(**a**), i.e., $Si_6O_n^+$(**a**) + O → $Si_6O_{n+1}^+$ (**a**). Therefore, the cationic silicon oxide clusters would be oxidized more efficient than neutral and anionic clusters.

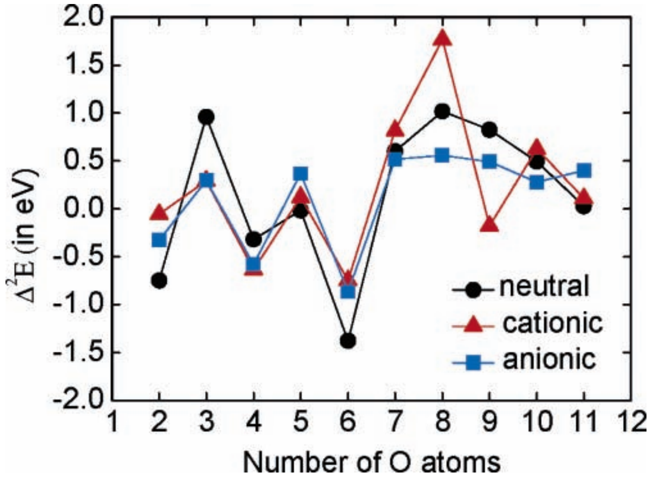

Figure 5. Second order differences in total energies by eq 4 for the lowest-energy structures of $Si_6O_n^{0,\pm}$(**a**) ($n = 2-11$) clusters, calculated at B3LYP/6-311G(2d).

C. Binding Energy and Fragmentation Energy. The relative stability of Si_6O_n, $Si_6O_n^+$, and $Si_6O_n^-$ ($n = 2-12$) clusters as a function of the O/Si ratio were investigated via the analysis of binding energies per oxygen atom $E_b(O)$, and second difference of total energies Δ^2E, which are defined by

$$E_b(O) = [E(Si_6) + n/2E(O_2) - E(Si_6O_n)]/n \quad (1)$$

$$E_b^+(O) = [E(Si_6^+) + n/2E(O_2) - E(Si_6O_n^+)]/n \quad (2)$$

$$E_b^-(O) = [E(Si_6^-) + n/2E(O_2) - E(Si_6O_n^-)]/n \quad (3)$$

$$\Delta^2E(Si_6O_n^{0,\pm}) = E(Si_6O_{n-1}^{0,\pm}) + E(Si_6O_{n+1}^{0,\pm}) - 2E(Si_6O_n^{0,\pm}) \quad (4)$$

In addition, fragmentation energies for neutral Si_6O_n clusters, defined by

$$E_{fragmentation}(Si_6O_n) = E(Si_6O_k) + E(Si_6O_l) - E(Si_6O_n), \quad (5)$$

were also calculated.

Figure 4 and Figure 5 show the $E_b(O)$ and Δ^2E curves with respect to the number of O atoms. We see from Figure 4 that the binding energy $E_b(O)$ reaches the maximum at $n = 8$, where O/Si ratio is about 1.3. Further increasing the number of O atoms in the cluster after $n = 8$ are not energetically favorable in E_b(O). In particular, the cationic clusters are less stable than the anionic clusters for n larger than 8. The special stability of Si_6O_8 can be also seen from the curve of second differences in total energies (Δ^2E) of Figure 5 which also shows a peak at Si_6O_8 and one at $Si_6O_8^+$. In addition, Si_6O_3 and Si_6O_5 are also shown to have a large stability, as seen from Figure 4 and Figure 5. Therefore, the Si-rich Si_6O_3 and Si_6O_5, and the O-rich Si_6O_8 clusters seem to be relatively stable clusters among the unsaturated Si_6O_n clusters. In contrast, Si_6O_6 and its ionic species are less stable as compared to their neighbors as we can see from the $E_b(O)$ curve of Figure 4 and Δ^2E curve of Figure 5,.

We have also calculated the fragmentation energies of Si_6O_n for various dissociation pathways. The results are shown in Table 1 and Figure 6. For Si_6O, Si_6O_3, and Si_6O_{7-11} clusters, the most favorable pathway is $Si_6O_n \rightarrow SiO + Si_5O_{n-1}$. On the other hand, Si_6O_2, Si_6O_4, Si_6O_5, and Si_6O_6 can dissociate into $Si_4 + Si_2O_2$, $Si_3 + Si_3O_4$, $Si_2 + Si_4O_5$, and $2Si_3O_3$, respectively. Besides SiO, other abundant oxide products in fragmentations are SiO, Si_2O_2, Si_3O_3, Si_3O_4, Si_4O_5, and Si_5O_{6-10}, which can be further dissociate into SiO pieces as we have shown previously.[10] The abundance SiO species in fragmentation of silicon oxide clusters is in consistent with the experimental results.[16,17] For Si_6O_{12}, the easiest fragmentation pathway is $Si_6O_{12} \rightarrow SiO_2 + Si_5O_{10}$, producing a SiO_2 molecule. It is clear from the calculated results of fragmentation energies (Figure 6) that Si_6O_{6-7} and Si_6O possess the smallest fragmentation energy, and thus can dissociate easily from thermodynamic viewpoint.

TABLE 1: Fragmentation Energies $E_{fragmentation}$ of Si_6O_n ($n = 1-12$) Neutral Clusters[a]

clusters	fragmentation channels	$E_{fragmentation}$ (in eV)
$Si_6O \rightarrow$	$Si_5 + SiO$	1.518
	$Si_4 + Si_2O$	3.644
$Si_6O_2 \rightarrow$	$Si_4 + Si_2O_2$	2.367
	$SiO + Si_5O$	2.662
$Si_6O_3 \rightarrow$	$SiO + Si_5O_2$	2.475
	$Si_3 + Si_3O_3$	2.625
$Si_6O_4 \rightarrow$	$Si_3 + Si_3O_4$	2.386
	$Si_3O + Si_3O_3$	2.451
$Si_6O_5 \rightarrow$	$Si_2 + Si_4O_5$	2.433
	$Si_3O + Si_3O_4$	2.532
$Si_6O_6 \rightarrow$	$Si_3O_3 + Si_3O_3$	0.732
	$Si + Si_5O_6$	1.555
$Si_6O_7 \rightarrow$	$SiO + Si_5O_6$	1.635
	$Si_2O_2 + Si_4O_5$	2.095
$Si_6O_8 \rightarrow$	$SiO + Si_5O_7$	2.578
	$Si_3O_3 + Si_3O_5$	4.462
$Si_6O_9 \rightarrow$	$SiO + Si_5O_8$	3.139
	$Si_2O_3 + Si_4O_6$	4.252
$Si_6O_{10} \rightarrow$	$SiO + Si_5O_9$	3.620
	$SiO_2 + Si_5O_8$	4.495
$Si_6O_{11} \rightarrow$	$SiO + Si_5O_{10}$	3.656
	$SiO_2 + Si_5O_9$	4.482
$Si_6O_{12} \rightarrow$	$SiO_2 + Si_5O_{10}$	4.491
	$Si_2O_4 + Si_4O_8$	4.846

[a] Fragmentation energies by eq 5 calculated at B3LYP/6-311G(2d).

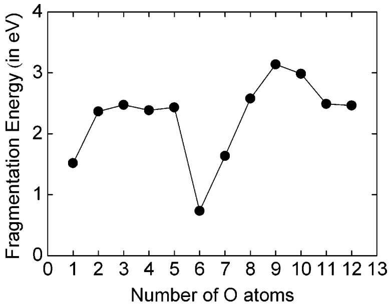

Figure 6. Fragmentation energies of Si_6O_n(**a**) clusters ($n = 1-12$) by eq 5, calculated at B3LYP/6-311G(2d).

It is interesting to note that for Si-rich clusters, e.g., Si_6O_{1-2} and Si_6O_{4-5}, the fragmentation products usually contain small pure Si clusters. Si_6O_3 can first dissociate into Si_5O_2 + SiO, of which Si_5O_2 can further dissociate into $Si_3 + Si_2O_2$.[10] Therefore, for the Si-rich clusters (Si_6O_{1-5}), there always exists a small Si fragment in the products of fragmentations. Such species of small Si_2, Si_3, Si_4, and Si_5 clusters dissociated from the Si-rich clusters may play a role in the growth of Si nanostructures in chemical vapor deposition method.

D. Electronic Properties. Figure 7 shows the HOMO−LUMO gaps of the neutral Si_6O_n clusters. For Si-rich cluster, the HOMO−LUMO gap scatters around 3 eV. Among the Si-rich clusters, Si_6O_3 has the smallest HOMO−LUMO gap of 2.54 eV, while Si_6O_4 has a larger gap of 3.98 eV. For the Si_6O_3, Si_6O_5, and Si_6O_8 clusters with large stability in energy as discussed above, the HOMO−LUMO gap of Si_6O_3 and Si_6O_5

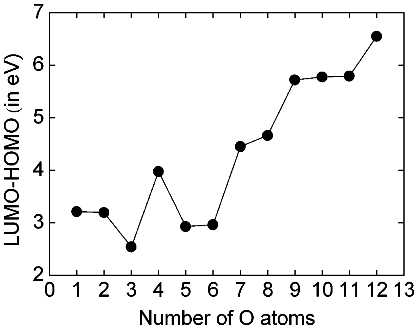

Figure 7. HOMO−LUMO gaps at B3LYP/6-311G(2d) for neutral Si_6O_n(**a**) ($n = 1-12$) clusters.

are much different from that of Si_6O_8, the former have the smaller gap and would be reactive, while the latter with the larger gap would be less reactive. For the clusters with O/Si close to 1, Si_6O_5 and Si_6O_6 have small HOMO−LUMO gaps, but there is a large increase in HOMO−LUMO gap from Si_6O_6 to Si_6O_7. For the O-rich clusters, the HOMO−LUMO gaps are larger with increasing O/Si ratio, and get at a maximum value at the end of O/Si = 2:1 ratio cluster Si_6O_{12}. From Si_6O_8 to Si_6O_{11}, the HOMO−LUMO gaps get a large increase from Si_6O_8 to Si_6O_9 and from Si_6O_{11} to Si_6O_{12}.

In silicon oxide systems, interaction between Si and O atoms will cause large charge transfer. Mülliken population analysis has been performed for some of the Si_6O_n clusters, and the results are shown in Figure 8. It is shown that there is a large charge transfer due to Si−O bonding, and Si atom in the clusters with 4-coordination by O atoms will possess largest charge. For the neutral Si-rich clusters, there is almost no charge transfer within the pure Si fragment, but there is large charge transfer within the silicon oxide fragment. For the ionic clusters $Si_6O_n^{\pm}$, the positive or negative charge is shown to be mainly carried by Si atoms for $n = 2-10$, but carried by both the boundary Si and O atoms for n = 11 and 12. From Figure 1 and Figure 2, the lowest-energy structures of the cationic clusters $Si_6O_n^+$ can often easily transform into the most favorable structures of neutral clusters Si_6O_{n+1}, e.g., $Si_6O_n^+$(**a**) + O → Si_6O_{n+1}(**a**) for n = 1, 2, 4, and 9. According to the Mülliken charge distributions, it is found that the position of the added O atom is likely at the Si atom with the largest positive charge.

IV. Conclusions

A systematic study of Si_6O_n clusters ($n = 1-12$) has been carried out at the DFT-B3LYP/6-311G(2d) level. Throughout an extensive search of lowest-energy structures, it has been found that for Si-rich clusters, the structural framework tends to consist of a pure Si fragment combined with an oxidized fragment. At O/Si ≈ 1:1 ratio, the Si atoms in the smaller silicon oxide clusters are almost completely oxidized. From Si_6O_9 to Si_6O_{10}, there exists an apparent structural motif transition from a disklike structure to a double-oxygen-bridged rod structure to accommodate more O atoms.

The ionic clusters $Si_6O_n^{\pm}$ have also been studied. The lowest-energy structures of the ionic clusters are mostly different from the lowest-energy structures of neutral clusters, except for the Si-rich cluster Si_6O_3 and the over-O-rich clusters Si_6O_{9-12}. The cationic $Si_6O_n^+$ clusters can easily transform continuously from one to another, i.e., $Si_6O_n^+$(**a**) + O → $Si_6O_{n+1}^+$(**a**).

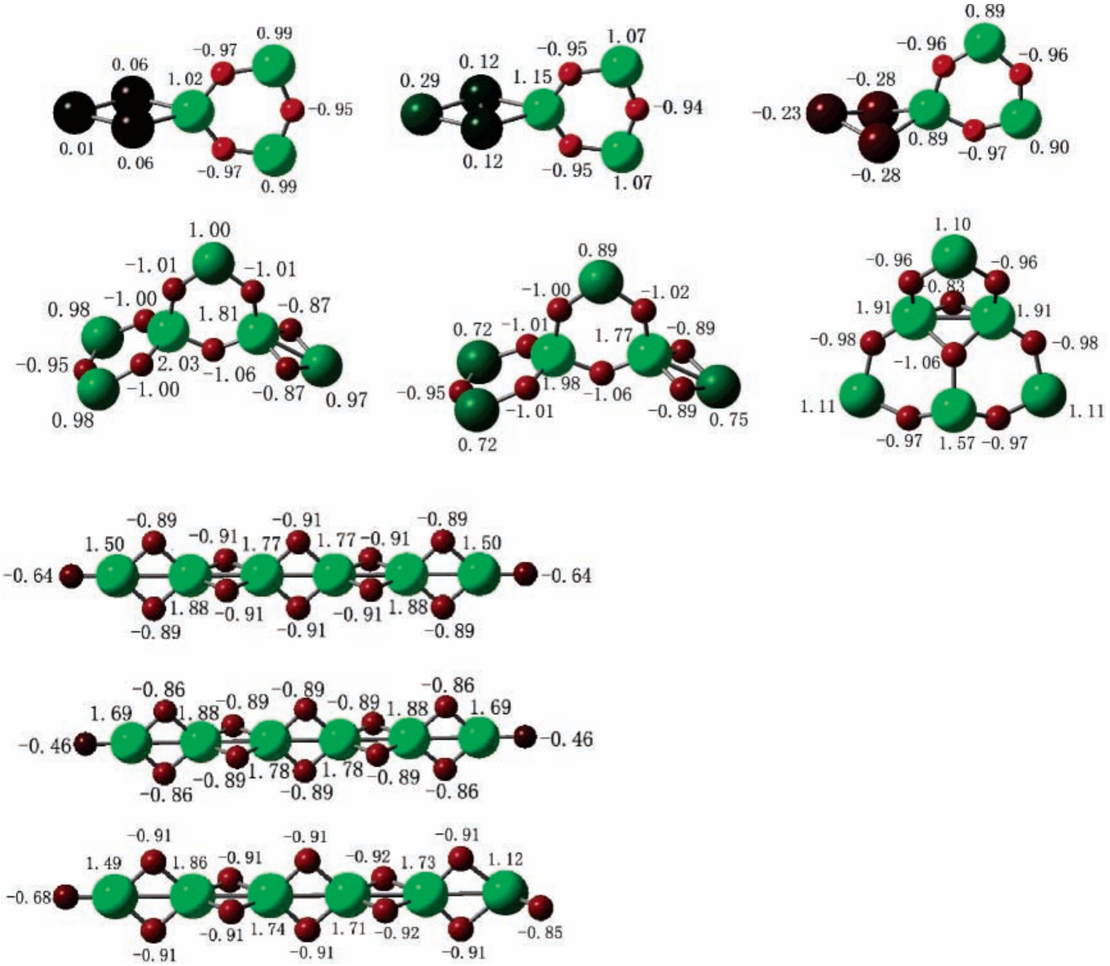

Figure 8. Mülliken charges of $Si_6O_{3,8,12}$ and their corresponding ionic structures. Big and small balls denote Si and O atoms, respectively.

From the binding energies and the second differences in total energies analysis, Si_6O_3 and Si_6O_5 are found to be stable species among Si-rich clusters, and Si_6O_8 acts as a stable species among the O-rich unsaturated clusters. Fragmentation study shows that there usually exists a smaller pure Si cluster in the fragmentation products for the Si-rich clusters. Another phenomenon we notice is that the O/Si = 1:1 ratio cluster (Si_6O_6) is the most unstable species which has the smallest second order difference in total energy and the smallest fragmentation energy, and can be considered as a transition point from the Si-rich to the O-rich clusters for Si_6O_n ($n = 1-12$) clusters.

Acknowledgment. This work is supported by Chinese Natural Science Foundation under Grant Nos. 20373009, 20473030, and 60028403. Ames Laboratory is operated for the U.S. Department of Energy by Iowa State University under Contract No. W-7405-Eng-82. This work was supported by the Director for Energy Research, Office of Basic Energy Sciences.

References and Notes

(1) Wang, L. S.; Nicholas, J. B.; Dupuis, M.; Wu, H.; Colson, S. D. *Phys. Rev. Lett.* **1997**, *78*, 4450.
(2) Wang, L. S.; Desai, S. R.; Wu, H.; Nichloas, J. B. *Z. Phys. D* **1997**, *40*, 36.
(3) Creasy, W. R.; O'Keefe, A.; McDonald, J. R. *J. Phys. Chem.* **1987**, *91*, 2848.
(4) Jarrold, M. F.; Ray U.; Creegan, K. M. *J. Chem. Phys.* **1990**, *93*, 224.
(5) Bergeron, D. E.; Castleman, A. W., Jr. *J. Chem. Phys.* **2002**, *117*, 3219.
(6) Torres, R.; Martin, M. *Appl. Surf. Sci.* **2002**, *193*, 149.
(7) Nath, K. G.; Shimoyama, I.; Sekiguchi, T.; Baba, Y. *Appl. Surf. Sci.* **2004**, *234*, 234.
(8) Torres, R.; Martin, M. *Appl. Surf. Sci.* **2002**, *193*, 149.
(9) Chelikowsky, J. R. *Phys. Rev. B* **1998**, *57*, 3333.
(10) Lu, W. C.; Wang, C. Z.; Nguyen, V.; Schmidt, M. W.; Gordon, M. S.; Ho K. M. *J. Phys. Chem. A* **2003**, *107*, 6936.
(11) Harkless, J. A. W.; Stillinger, D. K.; Stillinger, F. H. *J. Phys. Chem.* **1996**, *100*, 1098.
(12) Nayak, S. K.; Rao, B. K.; Khanna, S. N.; Jena, P. *J. Chem. Phys.* **1998**, *109*, 1245.
(13) Chu, T. S.; Zhang, R. Q.; Cheung, J. F. *J. Phys. Chem. B* **2001**, *105*, 1705.
(14) Avramov, P. V.; Adamovic, I.; Ho, K. M.; Wang, C. Z.; Lu, W. C.; Gordon, M. S. *J. Phys. Chem. A* **2005**, *109*, 6294.
(15) Lu, W. C.; Wang, C. Z.; Ho, K. M. *Chem. Phys. Lett.* **2003**, *378*, 225.
(16) Brewer, L.; Edwards, R. K. *J. Phys. Chem.* **1954**, *58*, 351.
(17) Porter, R. F.; Chupka, W. A.; Inghram, M. G. *J. Chem. Phys.* **1955**, *23*, 216.
(18) Bromley, S. T.; Zwijnenburg, M. A.; Maschmeyer, Th. *Phys. Rev. Lett.* **2003**, *90*, 035502.
(19) Bromley S. T.; Flikkema, E. *Phys. Rev. Lett.* **2005**, *95*, 185505.
(20) Zhang, R. Q.; Zhao, M. W.; Lee, S. T. *Phys. Rev. Lett.* **2004**, *93*, 095503.
(21) Frisch, M. J.; Trucks, G. W.; Schlegel, G. E.; et al. Gaussian 03, Revision B. 03, Gaussian, Inc.: Pittsburgh, PA, 2003.
(22) Becke, A. D. *J. Chem. Phys.* **1993**, *98*, 5648.